

Effects of inferior tibiofibular syndesmosis injury and screw stabilization on motion of the ankle: a finite element study

Qinghua Liu · Guanghui Zhao · Bin Yu ·
Jianbin Ma · Zhong Li · Kun Zhang

Received: 10 July 2013 / Accepted: 10 September 2014 / Published online: 19 September 2014
© European Society of Sports Traumatology, Knee Surgery, Arthroscopy (ESSKA) 2014

Abstract

Purpose Traditional studies of syndesmosis injury and screw stabilization have been conducted in cadaveric models, which cannot yield sufficient and exact biomechanical data about the interior of the ankle. The purpose of this study was to evaluate the effects of inferior tibiofibular syndesmosis injury (ITSI) and screw stabilization on the motion of the ankle with finite element analysis.

Methods Three-dimensional models of the ankle complex were created with CT images of a volunteer's right ankle in three states: normal, post-ITSI, and stabilization with a screw 2.5 cm above (parallel to) the ankle. Simulated loads were applied under three conditions: neutral position with single foot standing, internal rotation, and external rotation of the ankle.

Results Compared with the normal state, ITSI increased the relative displacement between the lower extremes of the tibia and fibula in the anteroposterior and mediolateral directions and the angular motion of the tibia, fibula, and talus at internal and external rotations (ERs). However, when stabilized with syndesmotic screws, the range

of motion (ROM) and all these parameters significantly decreased.

Conclusion ITSI can lead to internal and ER instability of the ankle joint. Screw stabilization is effective in controlling the instability, but may reduce markedly the ROM of the ankle joint. Through this study, it can be proposed that the screws should be removed once the healing is gained in order to restore normal function of the ankle joint as soon as possible.

Keywords Syndesmosis · Ankle · Finite element analysis · Internal fixation · Biomechanics

Introduction

The inferior tibiofibular syndesmosis is an important structure of the ankle mortise for weight transmission and walking [4, 7, 24]. Its injuries were reported to have accounted for about 1–11 % of all ankle lesions [6, 14]. However, in populations actively involved in sporting activities, the figure may be considerably higher.

There were different views on the effects of inferior tibiofibular syndesmosis injury (ITSI) on the ankle stability. Some reported that ITSI patients might develop subsequent chronic ankle instability [7], leading to persistent ankle pain and later traumatic arthritis, as well as complications such as anterior impingement syndromes of the ankle [9]. Likewise, Teramoto et al. [28] displayed that the injury led to inversion instability of the ankle joint. However, in a traditional biomechanical study by Boden et al. [4], disruption of the syndesmosis did not cause ankle instability if no medial injury was involved. Rasmussen et al. [23, 24] reported that cutting the syndesmosis increased only the external rotation (ER) instability.

Q. Liu · G. Zhao · J. Ma
Department of Joint Surgery, Hong-Hui Hospital, Xi'an Jiaotong University College of Medicine, 76 Nanguo Road, Beilin District, Xi'an 710054, China

B. Yu
Department of Orthopaedic Trauma, Nanfang Hospital, Southern Medical University, Guangzhou 510515, China

Z. Li · K. Zhang (✉)
Department of Orthopaedic Trauma, Hong-Hui Hospital, Xi'an Jiaotong University College of Medicine, 76 Nanguo Road, Beilin District, Xi'an 710054, China
e-mail: smu-liuqh@163.com

Syndesmotic injuries are graded from I to III, and therapeutic methods are varied accordingly [2]. Most syndesmosis injuries may be treated nonoperatively though recovery is frequently prolonged. Fixation of the distal fibula to the tibia is preferred for such severe injuries as studied in the present study, because it can maintain anatomical reduction and allow patients to resume weight-bearing activities. Of many methods to stabilize the disrupted syndesmosis, placement of a fully threaded transverse syndesmotic screw is recommended by AO as the ‘gold standard’ treatment [26]. It has been advised that the screw should be positioned between 2 and 3 cm proximal to the tibial plafond [25], but there has still been no consensus on issues regarding the syndesmotic screwing, such as optimal number of cortices, size of the screw, position of the foot during screw insertion, use of one or two screws, position of the screw(s) relative to the tibiotalar joint, use of bioabsorbable screws, time to weight bearing, or removal or not of the screw before weight bearing [29, 30].

Traditional research methods cannot reveal the force transmission mechanism at the interior of the ankle. For example, cadaveric specimens often have great individual differences and cannot display physiologic function. The finite element (FE) model studies have been recognized as reliable complementary tools for quantitative evaluation of biomechanical performance of tissues, organs, and articular joints [31]. Therefore, it is necessary to conduct FE analysis to explore the effects of ITSI and screw stabilization on the interior motion of the ankle. As the first attempt of such FE analyses, the present study aimed at exploring just the influence of screw stabilization on the motion of ankle joint using the 316 stainless steel screws of \varnothing 3.5 mm in fixation through the center of tibia and fibula on both sides. The biomechanical data from our FE models might provide theoretic evidence for clinical treatment of ITSI.

Materials and methods

Numerical approach and material models

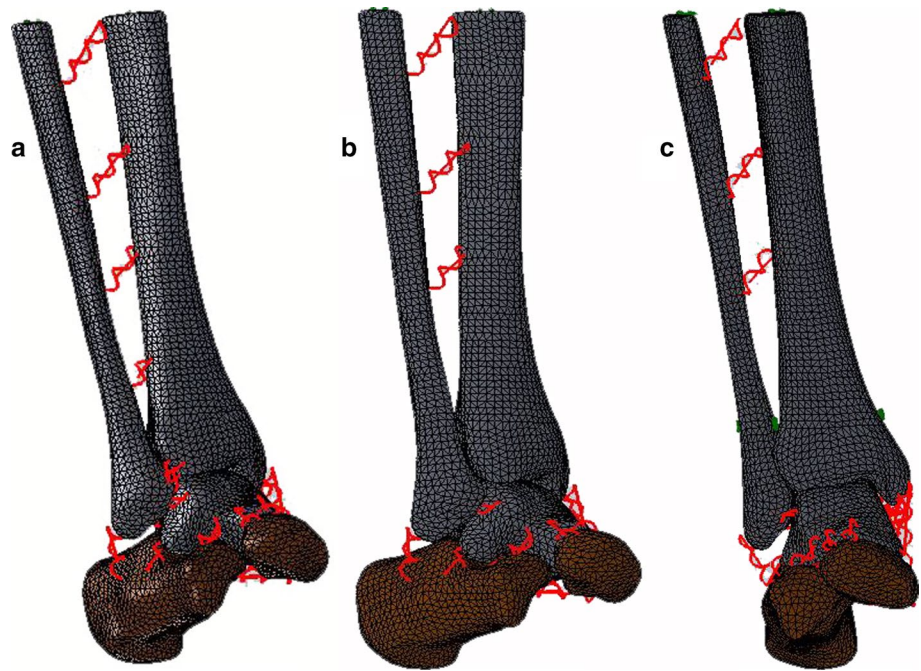
The geometrically accurate FE model was obtained from 3D reconstruction of the CT images of a male volunteer’s right foot and ankle (30 years, height 172 cm, body mass 60 kg) in the neutral unloaded position. This volunteer was free from previous trauma or any other abnormalities examined by radiograph. Cross-sectional CT images were taken with intervals of 0.6 mm from the plane 20 cm above the ankle down to the sole of the foot. Prior to radiography and CT scanning, informed consent was obtained from the volunteer after institutional review board (Hong-Hui Hospital, Xi’an Jiaotong University College of Medicine) approval.

Highly accurate boundary surfaces were fit to every bone using several automated and manual techniques available in Mimics (Materialise, Leuven, Belgium). Thresholding segmentation and region growing tools were used to reconstruct the 3D structures of the tibia, fibula, and talus of the ankle joint. Then, the data were exported in point cloud file format and transferred into SolidWorks 2009 (SolidWorks Corporation, Concord, MA, USA) to form geometric models, which were assembled together to construct the ankle complex with the tibia, fibula, talus, calcaneus, and navicular. The coordinate axes of the assembly were aligned so that the *X* axis pointed medially, the *Y* axis pointed posteriorly (toe to heel), the *XY* plane paralleled to the sole, and the *Z* axis pointed upward (heel to knee). Then, the data were imported into the Simulation module to establish a FE model of the ankle. Simulation allowed for the application of 3D contacts, springs, forces, and torques.

A new static example was created based on the assembly in the Simulation module. The bony structures were idealized as homogeneous, isotropic, and linearly elastic, with Young’s modulus and Poisson’s ratio assigned as 7,300 MPa and 0.3 [10], respectively. The parameters were selected according to cortical and trabecular elasticity [15]. Interactions among the five bones were defined as contact surfaces, which allowed relative articulating movement. Contact options were set as surface to surface and no penetration. Contacts between articular surfaces were considered frictionless, and gravity was considered negligible in the model, to simulate the lubricating nature of articular cartilage surfaces.

Linear and tension-only springs were used depending on their geometries to simulate ligaments’ connection. Attachment points on the bones were identified based on anatomical atlases [1], published data (Interactive foot and ankle, Primal Picture Limited, UK), and dissection. A total of 31 springs were included to simulate connected structures such as periarticular ligaments and the crural interosseous membrane. The distance between insertion sites in the neutral position (NP) were taken as initial ligament lengths. Ligaments with relatively big diameter-to-length ratios were represented by multiple elements according to literatures [16], to simulate the recruitment of ligament fibers under different loading conditions. Material properties of each ligament were determined by extensive references to literatures: The medial, lateral collateral ligaments of the ankle and the interosseous talocalcaneal ligaments were referred to the data by Siegle et al. [27]; the distal tibiofibular syndesmosis ligaments were referred to the data by Hoefnagels et al. [13] and Beumer et al. [3]. Other ligaments of which related data were not found in literature or varied greatly were all assumed to have a stiffness value between 70 and

Fig. 1 Three models of intact ankle (a), syndesmosis injuries (b), and screw fixation (c) were established, respectively



90 N/mm [17]. The crural interosseous membrane was represented by four springs (with a stiffness of 400 N/mm, determined by the lengths of the tibia and fibula, along with stiffness data found on the interosseous membrane of the forearm [21]). A pre-stretch (implemented by a reduction in zero-load length of 2 %) was applied to each ligament to represent in situ levels, and a pre-stretch value of 0.5 % was applied for the springs representing the interosseous membrane [17].

The ITSI model was simulated by suppressing the springs representing the anterior and posterior tibiofibular ligaments, the interosseous tibiofibular ligament, along with the distal interosseous membrane closest to the tibiotalar joint. The fixation model with screw was established for the final simulation. The screw was assumed as a simple cylinder with the threads ignored. A \varnothing 3.5-mm hole was generated on the plane 2.5 cm above the ankle mortise, in parallel to ankle articular surface and through the center of the fibula and tibia diaphysis. The cylindrical surfaces of the hole were connected to a 316 stainless steel pin on both sides, and the cylinder was fixed on the fibula and tibia to simulate the effect of the threaded section. Young's modulus and Poisson's ratio of the screw were defined as 1.9×10^5 MPa and 0.3, respectively.

Boundary conditions

Loadings at NP with single foot standing, internal rotation (IR), and ER of the ankle were simulated in all models. The

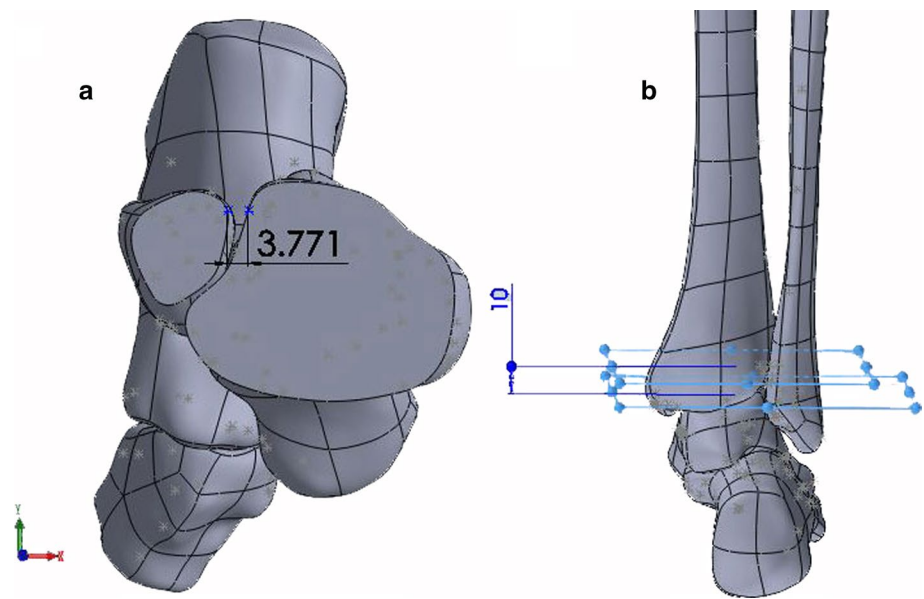
calcaneus and the navicular were fixed, and central points of the upper sections of the tibia and fibula were fixed while the remaining bones were free to move. A vertical force of 600 N was applied to the upper section of the tibia to simulate one foot balanced standing bearing a body mass of 60 kg. Then, a 67 N of compression load and a 2.7 N m of clockwise or counterclockwise torsional force were applied to the proximal tibia, to simulate internal and ER of the ankle, with the longitudinal axis of the tibia set as the rotation axis.

Mesh generation and solution

After these boundary conditions were set, the models were meshed with second-order 10-node tetrahedral elements by high-quality grid generation tool in the Simulation (Fig. 1). Grid density was set to "good," grid parameters to "normal grid," overall size to 2.8 mm, tolerance to 0.1 mm, and node of Jacobi to 4. Iteration computation was run by the Simulation automatic solver. All models mentioned above were in complete parallel.

The maximum displacement of the tibia and the fibula on the plane 1 cm proximal to the tibia plafond (Fig. 2) was measured in the anterior/posterior and medial/lateral directions [12]. Rotation angles of the bones were obtained by engineering graph generated in SolidWorks. More specifically, after the reference plane was paralleled to the tibiotalar joint surface and perpendicular to the longitude axis of the tibia which was determined as the rotation axis, the rotation angles were measured of the tibia, the fibula, and the talus, respectively (Fig. 3).

Fig. 2 The tibiofibular clear space of unloading model measured in this study [the distance between the lateral border of the posterior tibial tubercle and the medial border of the fibula (a), 10 mm proximal to the distal tibial articular surface (b)]



Results

Three models were established with a total number of elements ranged from 59,651 to 63,299 and nodes from 91,869 to 96,966, with 9 loadings conducted.

Translations of the tibia, the fibula, and relative to the tibia, in the anterior/posterior and medial/lateral directions

The maximum displacement values were compared among the models of ITSI, screw fixation, and the intact ankle. The translations of the fibula relative to the tibia increased significantly in contrast to the intact ankle in the medial/lateral and anterior/posterior directions after ITSI. The maximum translations were 4.6 mm in the medial/lateral directions and 2.0 mm in the anterior/posterior directions during the loading in the IR of the ankle. The translations were reduced significantly in various directions after screw stabilization of the syndesmosis (Fig. 4).

Rotation angles of the tibia, the fibula, and the talus, relative to the global coordinate system

Rotation angles of bones were calculated based on the angles between the unloading model and each loading model. It was shown that each bone rotation angle has changed significantly in ITSI, along with the increase of the range of motion (ROM). In the IR of the ankle, the ER angles of the tibia and the talus increased from 7.1° and 1.8° preinjury to 12.4° and 3.7° postinjury, respectively, while the rotation angle of the fibula changed from 3.4° ER to 1.1° IR. In the ER of the ankle, the IR angles of the tibia, the fibula, and the talus increased from 3.9°, 0.4° and 2.1°

to 5.5°, 1.1° and 2.4°, respectively. However, after screw stabilization of the tibiofibular syndesmosis, the rotation angles of both tibial and talus significantly decreased in comparison with the injury model. Compared to the intact model, the rotation angle of the talus increased in the IR and decreased in the ER of the ankle. The rotation angle of the fibula tended to be close to that of the tibia. The relative rotation angles of the tibiotalar joint increased from 5.3° in the intact model to 8.7° in the injury model and decreased to 1.8° in the screw fixation model in the IR of the ankle, and increased from 1.8° in the intact model to 3.1° in the injury model and decreased to 0.6° in the screw fixation model in the ER of the ankle (Fig. 5).

Discussion

The main finding of this study is that ITSI would lead to the increasing movement of the distal tibia and fibula. The anterior/posterior and medial/lateral displacements of the tibia and the fibula increased in coronal and sagittal planes of the human body during three loading conditions. Although the absolute distances in the inferior tibiofibular joint were widened during loading at standing in the NP and IR of the ankle, the tibiofibular clear space (TFCS) approached and exceeded the 6 mm criterion that was proposed by former researchers [12]. Besides, absolute distances were narrowed in the loading at ER of the ankle. This may be explained by the differences in research methods adopted. Furthermore, the results also indicated that the TFCS was associated with the loading state at the foot and ankle, which should be recognized in clinic.

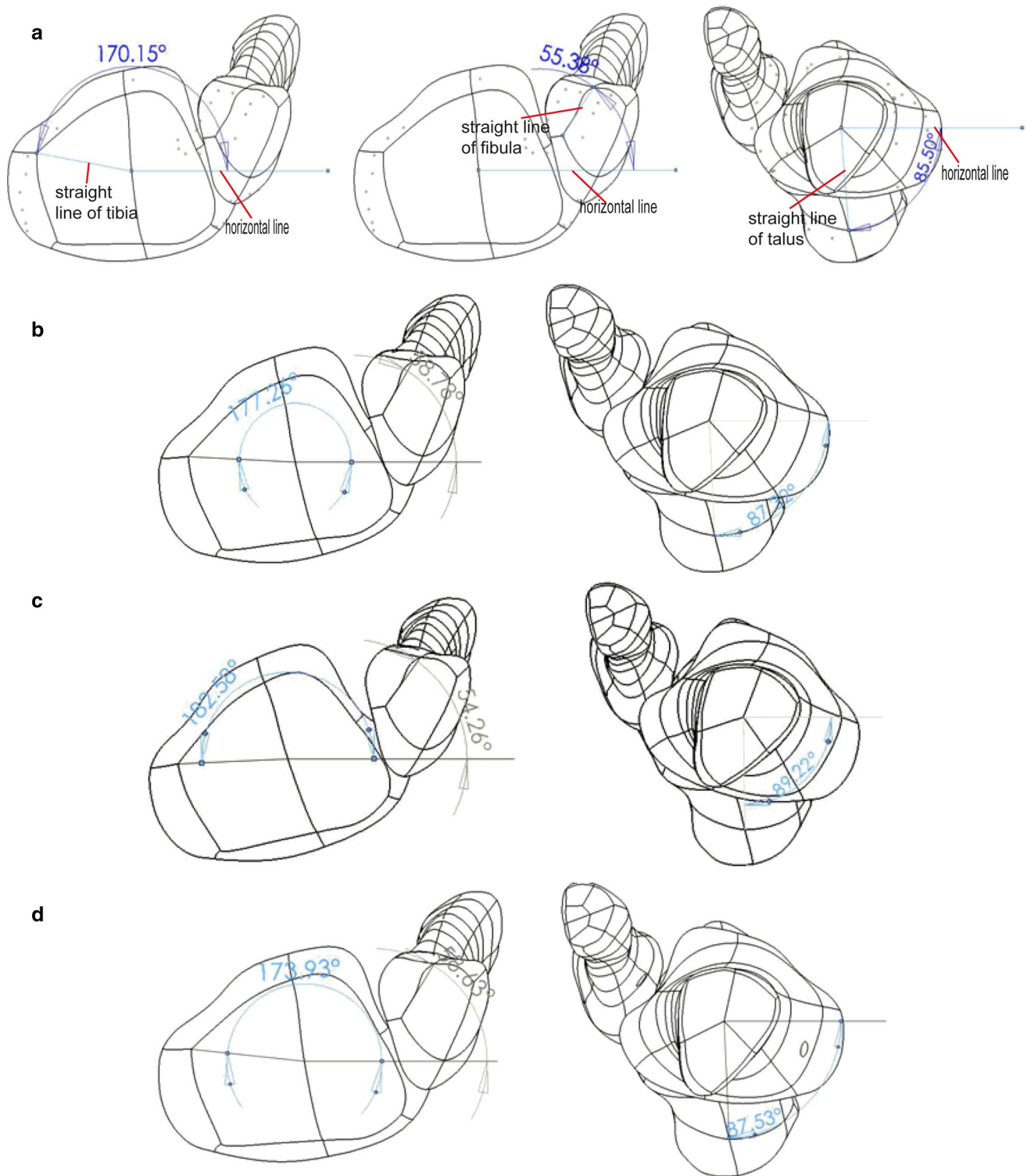


Fig. 3 Angles measured between the *horizontal line* and the *straight line* of tibia, fibula, and talus on the ankle plane in models before loading (a) and during internal rotation of the intact ankle (b), tibiofibular syndesmosis injury (c), and syndesmosis screw fixation (d)

Moreover, the present study showed that severe ITSI would cause the rotation angle of each bone of the ankle joint to increase in the internal and ERs of the ankle, so that

the ankle ROM was augmented. Therefore, severe syndesmosis injury causes not only ER instability of the ankle but also IR instability. Our study also demonstrated that after

Fig. 4 The maximal displacements and relative displacements of the tibia, the fibula at the plain 1 cm above the ankle joint surface, in the medial/lateral (a) and anterior/posterior directions (b), during application of neutral position (NP) with single foot standing, internal rotation (IR), and external rotation (ER) loads

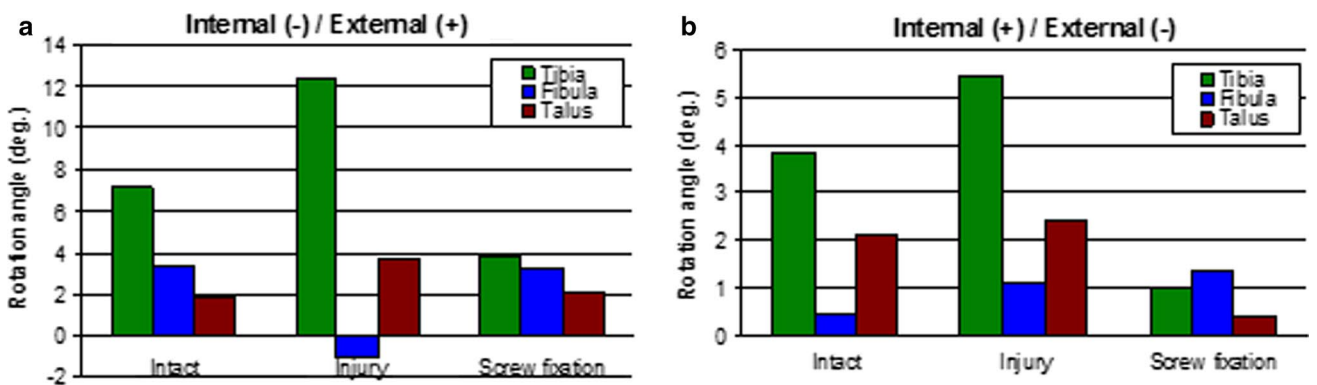
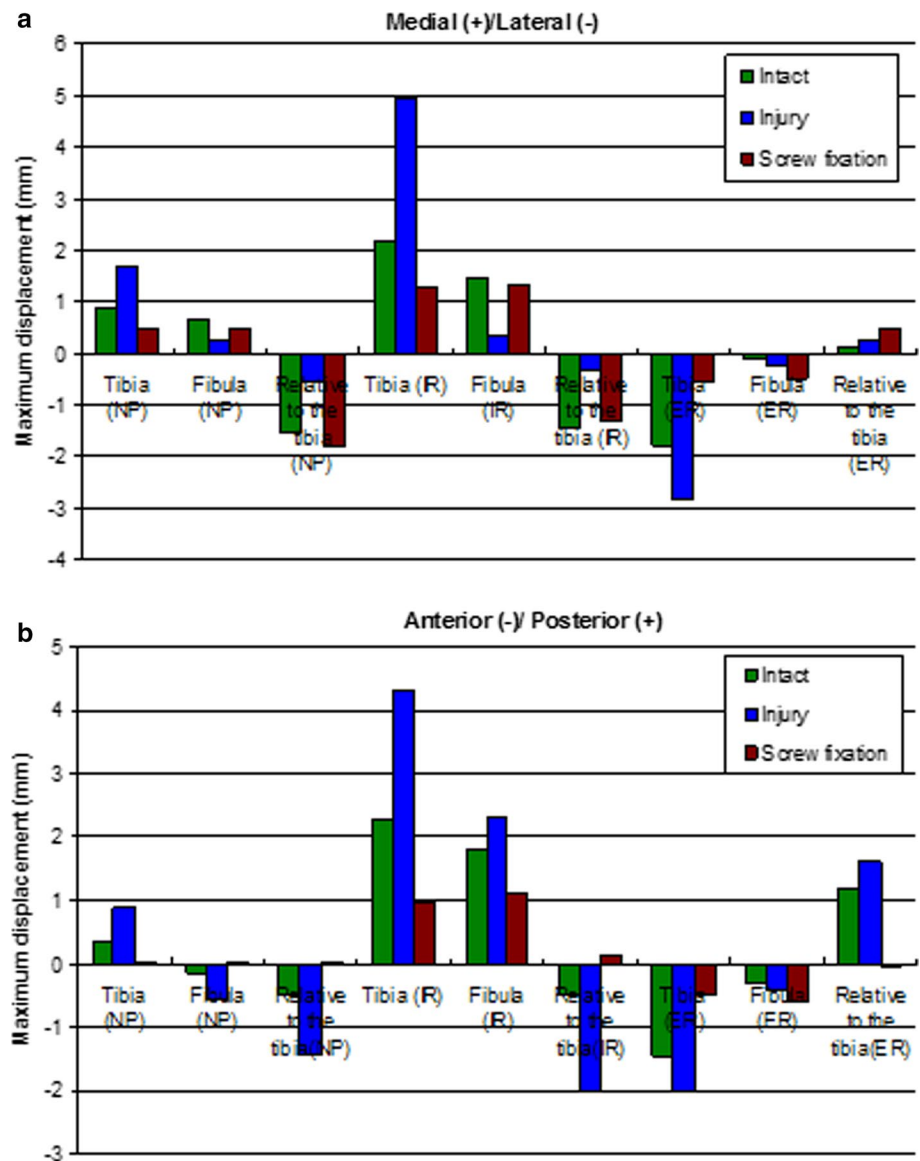


Fig. 5 The rotation angles of tibia, fibula, and talus during application of internal rotation (a) and external rotation (b) load in models of intact ankle, tibiofibular syndesmosis injury, and screw fixation

tibiofibular syndesmosis injury, the rotation angle of the talus increased by 1.9° and 0.3° during the IR and ER of the ankle, respectively, which were close to the results of the biomechanical study by Dolzynski et al. [8].

In an ideal treatment to ITSI, the implant should both stabilize the syndesmosis and allow physiologic micromotion as well as early mobilization, but this is hard to achieve, because instability at the injured site does not benefit early repair of soft tissues [5, 20, 22]. Effective conventional fixation for a period of time, however, can compromise the measure to promote scar healing of the syndesmosis. The present study showed that movements of the distal tibia and fibula decreased significantly in the anterior/posterior and medial/lateral directions after fixation with a syndesmosis screw. Absolute displacements were both <0.3 mm between the distal tibia and fibula. In addition, the rotation angles of the tibiotalar joint at the internal and ERs were significantly reduced. Meanwhile, the rotation angle of the fibula tended to be close to that of the tibia. Therefore, screw stabilization can provide a mechanically stable condition for the healing of the syndesmotic ligament complex.

However, a likely complication is that screw stabilization will still affect the ROM of the ankle joint even after the syndesmosis has gained healing in the long run. Moore et al. [19] and Hamid et al. [11] stated that retention of syndesmotic screws, even with mechanical failure, did not pose a clinical problem and weight bearing could be allowed at 6–10 weeks without routine removal of screws. Since the ultimate goal of treatment is to restore the joint function, we propose that the screws should be removed once the healing is gained in order to restore normal function of the ankle joint as soon as possible.

Despite some valuable results here obtained, the present study has limitations inherent in the modeling simplifications derived from several factors. Firstly, it is difficult in determining the typical values for mechanical characterization of materials when dealing with human tissues. Secondly, experimental studies have provided scarce data about characteristics of the ankle joint that can be used in our FE models. Thirdly, because a large number of non-linear problems are involved in the modeling and calculation, the convergence of results is also hard to control. As a result, bones are considered homogeneous, isotropic, and linearly elastic. Ligaments are represented as linear springs, in an attempt to replicate the behavior associated with the linear region of ligament tensile behavior. Articular cartilage deformation is neglected as the bones are represented by rigid objects; cartilage function is incorporated by neglecting friction in the model. These and other limitations of the present models, such as simplified screw geometry, the parameters of the models' grid, must be taken into account before a direct translation of these data into a clinical situation. However, the results of this research were

mainly obtained by calculating the data of displacement distribution from the models, which are relatively closer to the actual ones than the stress values. The latter are influenced greatly by such factors as the grid size of a model and generally present a qualitative result. The displacement values of each bone might reflect more accurately the motion of the ankle joint. In our previous work [18], the FE models established had been compared with Liacouras and Wayne's for the purpose of model validation. Overall, the findings of this study are helpful in guiding the clinical diagnosis and management of tibiofibular syndesmosis injuries.

Conclusion

The present FE analysis shows that severe syndesmosis injury causes not only ER instability but also IR instability of the ankle. Therefore, reduction and operative stabilization are necessary. Although a transverse syndesmotic screw can effectively control excessive abnormal activity of the distal tibia and fibula following tibiofibular syndesmosis injury, the screw fixation affects the physiologic normality of the joint, leading to decreased magnitude of displacement at the lower extreme of tibia and fibula and decreased ROM of the articulation.

Acknowledgments This work was supported by the Shaanxi Province Science Technology Research and Development Projects (No. 2011K12-05-13) and the Natural Science Foundation of China (No. 81071233). We also thank Professor Liang Allen Ping and Ms Zhang Yifang for their revision and editing of this manuscript.

Conflict of interest The authors declare that they have no conflict of interest.

References

1. Agur A, Lee M (1999) Grant's atlas of human anatomy, 10th edn. Lippincott Williams and Wilkins, Philadelphia
2. Bauer AS, Blumanb EM, Wilsona MG, Chiodoa CP (2009) Injuries of the distal lower extremity syndesmosis. *Curr Orthop Pract* 20:111–116
3. Beumer A, van Hemert WL, Swierstra BA, Jasper LE, Belkoff SM (2003) A biomechanical evaluation of the tibiofibular and tibiotalar ligaments of the ankle. *Foot Ankle Int* 24:426–429
4. Boden SD, Labropoulos PA, McCowin P, Lestini WF, Hurwitz SR (1989) Mechanical considerations for the syndesmosis screw. A cadaver study. *J Bone Joint Surg Am* 71:1548–1555
5. Bray RC, Shrive NG, Frank CB, Chimich DD (1992) The early effects of joint immobilization on medial collateral ligament healing in an ACL-deficient knee: a gross anatomic and biomechanical investigation in the adult rabbit model. *J Orthop Res* 10:157–166
6. Cedell CA (1975) Ankle lesions. *Acta Orthop Scand* 46:425–445
7. Close JR (1956) Some applications of the functional anatomy of the ankle joint. *J Bone Joint Surg Am* 38:761–781

8. Dotzyński M, Latosiewicz R (1998) Rotatory instability of the ankle: an experimental investigation of tibio-fibular syndesmosis function. *Chir Narzadow Ruchu Ortop Pol* 63:451–454
9. Gardner MJ, Demetrakopoulos D, Briggs SM, Helfet DL, Lorich DG (2006) Malreduction of the tibiofibular syndesmosis in ankle fractures. *Foot Ankle Int* 27:788–792
10. Gefen A, Megido-Ravid M, Itzhak Y, Arcan M (2000) Biomechanical analysis of the three-dimensional foot structure during gait: a basic tool for clinical applications. *J Biomech Eng* 122:630–639
11. Hamid N, Loeffler BJ, Braddy W, Kellam JF, Cohen BE, Bosse MJ (2009) Outcome after fixation of ankle fractures with an injury to the syndesmosis: the effect of the syndesmosis screw. *J Bone Joint Surg Br* 91:1069–1073
12. Harper MC, Keller TS (1989) A radiographic evaluation of the tibiofibular syndesmosis. *Foot Ankle* 10:156–160
13. Hoefnagels EM, Waites MD, Wing ID, Belkoff SM, Swierstra BA (2007) Biomechanical comparison of the interosseous tibiofibular ligament and the anterior tibiofibular ligament. *Foot Ankle Int* 28:602–604
14. Hopkinson WJ, St Pierre P, Ryan JB, Wheeler JH (1990) Syndesmosis sprains of the ankle. *Foot Ankle* 10:325–330
15. Huiskes R (1982) On the modeling of long bones in structural analyses. *J Biomech* 15:65–69
16. Imhauser CW, Siegler S, Udupa JK, Toy JR (2008) Subject-specific models of the hindfoot reveal a relationship between morphology and passive mechanical properties. *J Biomech* 41:1341–1349
17. Liacouras PC, Wayne JS (2007) Computational modeling to predict mechanical function of joints: application to the lower leg with simulation of two cadaver studies. *J Biomech Eng* 129:811–817
18. Liu Q, Zhang K, Zhuang Y, Li Z, Yu B et al (2013) Analysis of the stress and displacement distribution of inferior tibiofibular syndesmosis injuries repaired with screw fixation: a finite element study. *PLoS ONE* 8:e80236
19. Moore JA Jr, Shank JR, Morgan SJ, Smith WR (2006) Syndesmosis fixation: a comparison of three and four cortices of screw fixation without hardware removal. *Foot Ankle Int* 27:567–572
20. Ogata K, Whiteside LA, Andersen DA (1980) The intra-articular effect of various postoperative managements following knee ligament repair: an experimental study in dogs. *Clin Orthop Relat Res* 150:271–276
21. Pfaeffle HJ, Tomaino MM, Grewal R, Xu J, Boardman ND et al (1996) Tensile properties of the interosseous membrane of the human forearm. *J Orthop Res* 14:842–845
22. Qamar F, Kadakia A, Venkateswaran B (2011) An anatomical way of treating ankle syndesmotom injuries. *J Foot Ankle Surg* 50:762–765
23. Rasmussen O (1985) Stability of the ankle joint. Analysis of the function and traumatology of the ankle ligaments. *Acta Orthop Scand Suppl* 211:1–75
24. Rasmussen O, Tovborg-Jensen I, Boe S (1982) Distal tibiofibular ligaments. Analysis of function. *Acta Orthop Scand* 53:681–686
25. Ruedi TP, Murphy WM (2000) AO principles of fracture management. AO Publishing, New York
26. Schepers T (2012) Acute distal tibiofibular syndesmosis injury: a systematic review of suture-button versus syndesmotom screw repair. *Int Orthop* 36:1199–1206
27. Siegler S, Block J, Schneck CD (1988) The mechanical characteristics of the collateral ligaments of the human ankle joint. *Foot Ankle* 8:234–242
28. Teramoto A, Kura H, Uchiyama E, Suzuki D, Yamashita T (2008) Three-dimensional analysis of ankle instability after tibiofibular syndesmosis injuries: a biomechanical experimental study. *Am J Sports Med* 36:348–352
29. van den Bekerom MP, Hogervorst M, Bolhuis HW, van Dijk CN (2008) Operative aspects of the syndesmotom screw: review of current concepts. *Injury* 39:491–498
30. van den Bekerom MP, Lamme B, Hogervorst M, Bolhuis HW (2007) Which ankle fractures require syndesmotom stabilization? *J Foot Ankle Surg* 46:456–463
31. Xu C, Zhang MY, Lei GH, Zhang C, Gao SG et al (2012) Biomechanical evaluation of tenodesis reconstruction in ankle with deltoid ligament deficiency a finite element analysis. *Knee Surg Sports Traumatol Arthrosc* 20:1854–1862